Desalination and Water Treatment
www.deswater.com
doi: 10.5004/dwt.2020.25669

201 (2020) 1–12
October

Forward osmosis by introducing temperature responsive poly(propylene fumarate-*co*-N-vinyl pyrrolidinone) hydrogel as a new draw solute

Ali Borsalani, Seyed Mostafa Tabatabaee Ghomsheh*, Masoomeh Mirzaei, Alireza Azimi

Department of Chemical Engineering, Mahshahr Branch, Islamic Azad University, Mahshahr, Iran,
emails: Mostafa.tabatabaee@yahoo.com (S.M.T. Ghomsheh), borsalani.ali1397@yahoo.com (A. Borsalani),
Mirzaei_fateme@yahoo.com (M. Mirzaei), Alireza_azimi550@yahoo.com (A. Azimi)

Received 4 July 2019; Accepted 24 January 2020

ABSTRACT

Forward osmosis (FO) is an emerging technology for water desalination which requires no external force for its operation. The performance of FO for water desalination is dependent on draw solution (DS) that must provide high osmosis pressure, minimum reverse flux, and efficient separation of water. The purpose of this study was to evaluate and characterize the novel temperature responsive hydrogel of poly(propylene fumarate-*co*-N-vinyl pyrrolidinone) that can be used as a new draw agent in the forward osmosis process of desalination. These hydrogels were synthesized using the copolymerization method. By considering the initial PPF/NVP mole ratios, copolymers were synthesized to have their own distinctive volume phase transition temperature which was established using differential scanning calorimetry. Also, these hydrogels were systematically investigated by using scanning electron microscopy and Fourier transform infrared spectroscopy. The swelling ratios of the hydrogels at different temperatures were measured. Furthermore, the deswelling kinetics of the hydrogels was also studied by measuring their water retention capacity. The osmotic pressure, relative viscosity, and FO performance of poly(PPF-*co*-NVP) draw solutions with different concentrations are studied systematically. It is found that the osmotic pressure and water flux of the novel DS are directly dependent on the concentration of hydrogels. This work proposes an innovative temperature responsive material as the draw solution having some functions, that is, high osmotic pressure, low salt leakage, high generated flux, and efficient recovery by temperature difference. So, the excellent performance and available recovery route of the developed poly(PPF-*co*-NVP) hydrogels as the draw solutions imply their great potential as promising draw solutions for FO applications.

Keywords: Forward osmosis; Hydrogel; Poly(propylene fumarate); Poly(N-vinyl pyrrolidinone); Copolymer

1. Introduction

Forward osmosis (FO) is a novel membrane-based technology for water desalination. It has gained increasing attention from industries because of its ability at the low operating cost compared to traditional processes [1–5]. In the FO process, the osmotic pressure difference between two sides of the semipermeable membrane is employed as the driving force for water to permeate from the draw solution to the feed solution. Its low fouling tendency and high separation efficiency gain valuable advantages as a promising water treatment technology [6]. Despite the advantages of the FO process, the performance and practical applications of FO technology are affected by suitable FO membranes and draw solutions [7–9]. Recently, considerable efforts have focused on developing a novel draw solution [10–12]. An appropriate draw agent should possess a high enough osmotic pressure relative to the feed

* Corresponding author.

solution, which is required to induce a high flux in the FO step. Also, low reverse salt diffusion and easy recovery of the diluted draw solution are other basic criteria for selecting suitable draw solutions in the FO process [13]. As yet the number of research publications on the FO process has increased, more efforts have been focused on the development of new membranes and process performance and this is while the exploration of the appropriate draw solutes is relatively limited [14]. Inorganic salts [15–17] are mostly studied draw solutions, which can create reasonable water flux but exhibit a severe reverse salt flux [6]. However, their large-scale applications are severely constricted due to the high amount of energy cost required to recover the draw solution with current technologies [18]. Salt leakage and recovery are two main problems associated to draw solutions. In recent years, synthetic draw solutes with the controllable molecular size have been fabricated to solve these problems, including polyelectrolyte of polyacrylic acid sodium salts [19], switchable polarity solvents [20,21], carboxyethyl amine sodium salts (CASSs) [8], and so on. Recently the new class of draw solute (DS), the polymer hydrogel particles for FO applications are considered.

Hydrogels are formed by crosslinking polymer chains through physical, ionic, or covalent interactions that are insoluble but have the ability to absorb large amounts of water within three-dimensional polymer networks. The polymer network has the strong ability to absorb a large amount of water with the designed shape of polymer that retained in a reasonable shape [22].

In particular, hydrogels with ionic groups on the comonomer unit are able to attract even greater amounts of water, this increased osmotic pressure arising because the covalently-incorporated ionic groups are balanced by mobile counter ions, and these counter ions provide a positive osmotic pressure inside the hydrogel which drives greater water sorption [23].

One main characteristic of polymer hydrogels is that they can undergo reversible volume change or solution–gel phase transitions in response to environmental stimuli such as temperature, light, pressure, or even pH. One particular interesting response to these stimuli is the change from hydrophilic to hydrophobic (generated physical and chemical stimuli), which induces hydrogel particles to release water.

This project aimed to develop a novel DS reversible temperature-responsive poly(propylene fumarate-*co*-N-vinyl pyrrolidinone) hydrogel to apply in FO process for producing potable water. The novel DS does not only have high osmotic pressure to develop a high water flux across the FO membrane, but also possesses a high absorption capability upon temperature difference to separate product water and regenerate the draw solution.

In this study effects of the solution concentration on the osmotic pressure, viscosity, and the resultant FO performance of the draw solutions are studied systematically. The potential desalination application is also explored.

2. Materials and methods

2.1. Materials

Diethyl fumarate (≥99%) and propylene glycol (≥98%) were purchased from QRec. Zinc chloride (≥97%), methylene chloride (≥99%), and 2-propanol (≥98%) were purchased from Loba Chemie Pvt. Ltd., India. Poly N-vinyl pyrrolidinone (≥99%) was supplied from Sigma Aldrich, India. Poly (methyl methacrylate) (MMA, ≥99%) as a cross linker, benzoyl peroxide (BP, ≥98%) as an initiator and N,N-dimethyl-p-toluidine (DMT, ≥98%) as an accelerator agents were purchased from Sigma–Aldrich (Steinheim, Germany). All the chemicals were used without further purification.

2.2. Gel synthesis and characterization

The synthesis of PPF has been previously described [24]. Briefly, diethyl fumarate was vigorously mixed with a three-fold molar excess of propylene glycol at 160°C in the presence of hydroquinone and zinc chloride. The reaction was performed under a nitrogen blanket. Transesterification of the intermediate fumaric diester was performed at 150°C under a vacuum of approximately 115 mm Hg under vigorous stirring. The byproduct ethanol and propylene glycol were removed by distillation under nitrogen. Poly(N-vinyl pyrrolidinone) was added to the reaction vessel under the same conditions to form the copolymer. The resulting copolymer was precipitated from methylene chloride with 2-propanol. The copolymer was recovered with a separation funnel and dried under reduced pressure. The molecular weight of the purified copolymer was determined by gel permeation chromatography (GPC) (CTO-10ASVP, Shimadzu, Japan) using polystyrene standards for a universal calibration curve as previously described [25].

Cross-linked copolymer networks were fabricated using a poly(methyl methacrylate) (MMA) as a cross linker, benzoyl peroxide (BP) as a initiator, and N,N-dimethyl-p-toluidine (DMT) as an accelerator agents.

The presence of functional groups in synthetic hydrogel samples were assessed by Fourier transform infrared spectroscopy (FTIR) using a Thermo Scientific Nicolet 6700 FTIR spectrometer (Waltham, MA, USA) (in the range of 500–4,000 cm^{-1}). FTIR is used to obtain the infrared spectrum of for a particular sample. It collects data over a wide spectral range, and this data can be used to identify specific functional groups that are present in the sample being studied. Spectral outputs were recorded in transmittance mode as a function of wave number.

The specific surface area (Brunauer–Emmett–Teller (BET)), pore volume, and pore size distribution were measured by nitrogen adsorption–desorption measurements using Micrometrics, ASAP 2020, surface area, and porosity analyzer (USA).

The internal pore structures of the hydrogels were characterized using KYKY EM3200 instrument with an accelerating voltage of 27 kV. For preparation of the morphology images the hydrogels which were under equilibrium in distilled water were quenched and freezed in a deep freezer and then the gels were lyophilized for 10 h to completely dehydrate without disturbing the internal pore structure of the hydrogel. The samples were then coated with a thin film of gold.

The effect of N-vinyl pyrrolidinone on the volume phase transition temperature (VPTT) of hydrogel was investigated using DSC-60A (Shimudza Company, Japan). Experiment was conducted under a constant flow rate (50 mL/min) of

nitrogen purge gas and the dried sample was heated from 0°C to 70°C at 10°C/min followed by cooling to 0°C at the same rate.

The swelling ratios of hydrogels were measured gravimetrically in the controlled temperature range of 15°C–50°C in water bath. Initially Gel samples were incubated in DI water for at least 24 h at room temperature. The temperature of the distilled water was increased to 50°C. After it reaches equilibrium at that particular temperature, the hydrogel was removed from the bath and the weight of the gel was recorded at 5°C intervals after blotting the excess surface water with moistened Whatman #1 filter paper. The dry weight of the hydrogel was measured after drying it under vacuum at room temperature. The equilibrium swelling ratio was calculated by following equation [26]:

$$\text{Equilibrium swelling ratio} = \left(\frac{W_w - W_d}{W_d} \right) \tag{1}$$

where W_w and W_d are the weights of hydrogel at equilibrium swelling and dry state, respectively.

The kinetics of deswelling of the hydrogels was measured gravimetrically after a temperature jump from the equilibrated swollen state at 20°C to the hot DI water at 50°C was measured after wiping off the excess water on the surface with moistened filter paper.

The weight changes were recorded during the shrinking course at regular time intervals until the weight remained invariant.

The deswelling ratio is defined as follows [27]:

$$\text{DS} = \frac{W_t - W_d}{W_s} \tag{2}$$

where W_t is the weight of the wet hydrogel at regular time intervals, W_s is the weight of the water in the swollen gel and W_d is the dry weight of the gel. The deswelling kinetics of the hydrogels at 50°C would be obtained by the relation curve of DS and time.

2.3. Draw solution characteristics affecting FO process performance

A high-efficient FO process is mainly affected by several essential factors. These factors are, in general, related to the membrane performance, suitable draw solution, and operating conditions. The primary characteristics essential for any draw solution is high osmotic pressure, much higher than the feed solution. The osmotic pressure of the ideal dilute solution is defined based on the theory proposed by van't Hoff as shown below [28]:

$$\pi = n\left(\frac{c}{M_w} \right) RT \tag{3}$$

where n is the number of moles of species formed by the dissociation of solutes in the solution, c is the solute concentration in g/L of solution, M_w is the molecular weight of the solute, R is the gas constant (R = 0.0821), and T is the absolute temperature of the solution.

Relative viscosities (η_R) of draw solutions against DI water with a concentration range of 0–2.5 M were tested in 25°C by using Eq. (4) [6]:

$$\eta_R = \frac{\eta_{\text{salt}}}{\eta_{\text{water}}} = \frac{t_{\text{salt}}\rho_{\text{salt}}}{t_{\text{water}}\rho_{\text{water}}} \tag{4}$$

where t_{salt} and t_{water} (s) are the respective outflow time of the draw solution and DI water, determined using a commercial Ubbelohde viscometer with temperature maintained by a water bath, their densities, were measured by a portable density meter (DMA 35, India). In addition, the performance of FO process is however affected by draw solution concentration.

Most studies have shown that higher water fluxes can be achieved by increasing the draw solution concentration. However, contrary to the theoretical solution-diffusion model, which establishes a linear relation between water fluxes and draw solution concentration, experiments have shown that this relation is non-linear. Linear relation is observed at lower concentrations, but at higher draw solution concentration, a logarithmic relationship has been visually observed [29–32].

2.4. Experiment setup

The membrane that used in this work was a commercial flat-sheet cellulose triacetate (CTA) FO membrane, which was purchased from Hydration Technology Innovations (Albany, USA). The FO system in a laboratory-scale cross-flow test unit was equipped with two peristaltic pumps (BT00–600M, Changzhou Kejian Peristaltic Pump Co.), tank (Super Duplex stainless steel) for feed, two water baths to control the temperature at 25°C ± 0.5°C, draw solution container, membrane chamber, and membrane inlet and outlet gauge pressure. The membrane cell is of an effective membrane area of 20.8 cm^2. Feed tank that is capable of holding about 20 L of the solution was placed on a digital scale (BW12KH, Shimadzu, Japan) and the feed solutions on both sides of the FO membrane was circulated using peristaltic pump. FO tests were performed at 25°C under FO mode (feed solution toward the skin layer of the membrane).

2.5. FO experiments

A laboratory-scale cross flow FO membrane test unit was used for the FO experiments. Theoretical water flux (J_w (LMH)) across the FO membrane was calculated from the volume change of feed solution following Eq. (5):

$$J_w = \frac{\Delta V}{A\Delta t} \tag{5}$$

where ΔV (L) is the volume change of feed solution over a predetermined time Δt (h), and A is the effective FO membrane surface area (m^2).

The reverse solute flux (RSF) (J_s) of a draw solute can be calculated from the increase of the DS concentration in the feed solution [33]:

$$J_s = \frac{(C_t V_t) - (C_0 V_0)}{\Delta t} \frac{1}{A_m} \quad (6)$$

where C_t (g/L) and V_t (L) are the salt concentration and feed volume at a time t, C_0 (g/L), and V_0 (L) are the salt concentration and feed volume at t_0, $\Delta t = t - t_0$ (h) is the duration of the experiment and A_m (m^2) is the effective membrane area.

RSF of the DS can not only decrease the performance of the process by decreasing the net osmotic pressure across the membrane, but can also complicate concentrate management. The accumulation of draw solute in the feed solution can also have adverse effect on sensitive receiving environment or alter adjacent treatment processes.

3. Results and discussion

3.1. Characterization of poly(PPF-co-NVP) synthetic gel

Poly(PPF-*co*-NVP) hydrogel was synthesized at various molar ratios of PPF and NVP. Schematic representation of synthesis is illustrated in Fig. 1. The PPF and NVP molar ratio were varied from 90:10 to 60:40. In all the formulations, the gelation process took place within seconds after the addition of initiator, and the gelation time of copolymer increases with increasing NVP concentration which was observed visually. The digital images of the synthesized hydrogels at room temperature are shown in Fig. 2.

Visual observation of the synthesized hydrogel demonstrated that the physical stability of hydrogel decreased as NVP concentration increased. However, hydrogel synthesized using 60:40 molar ratio was too slimy with low mechanical stability and ruptured upon swelling and hence 60:40 molar ratio was not further consider for the hydrogel synthesis.

Decreasing of hydrogel physical stability by NVP concentration increasing was observed.

The molecular weights of the copolymers are shown in Table 1. All data of this Table were obtained by GPC. Number average molecular weight (M_n) and weight average molecular weight (M_w) were based on polystyrene standards in chloroform.

Fig. 3 shows the FTIR spectrum of PPF, NVP, and Poly (PPF-*co*-NVP). The peaks located at 1,647; 1,426; and 1,279 cm^{-1} for NVP are assigned to the C=O stretching vibration, CH_2 bending vibration, and C–N stretching vibration band, respectively. For PPF the ester carbonyl bonds and C=C stretching appeared at 1,726 and 1,646 cm^{-1}, respectively. in the spectrum of Poly(PPF-*co*-NVP) the broad absorption picks around 1,662 and 1,720 cm^{-1} can be attributed to the −C=O– stretching vibration of NVP and fumarate, respectively. Also this spectrum showed the disappearance of a peak at 1,646 cm^{-1} due to cross-linking at the −CH=CH− group.

The surface area and pore structure of synthetic hydrogels were determined by employing the nitrogen isothermal adsorption technique (BET method). The nitrogen adsorption–desorption isotherms and pore size distributions of synthetic hydrogels are represented in Figs. 4 and 5. These isotherms display type IV isotherms with *H*3 hysteresis loops, characteristics of mesoporous materials. The textural properties of prepared hydrogels are also systematically shown in Table 2. As can be seen, the addition of increase content of NVP over synthetic hydrogels caused a decrease in average pore diameter. Furthermore; it is remarkable to note that, surface area increases, and pore volume decreases as content of NVP increases. The interfacial interactions between PPF and NVP hydrogel have great influence on pore structure of the hydrogels as evident from this study.

Fig. 6 shows the SEM images for the freeze-dried hydrogels. As can be seen, pore structure of hydrogels has increased by incorporation of NVP. The addition of NVP provides more pores and interconnectivity between the pores. So this structural modification has increased hydrophilicity

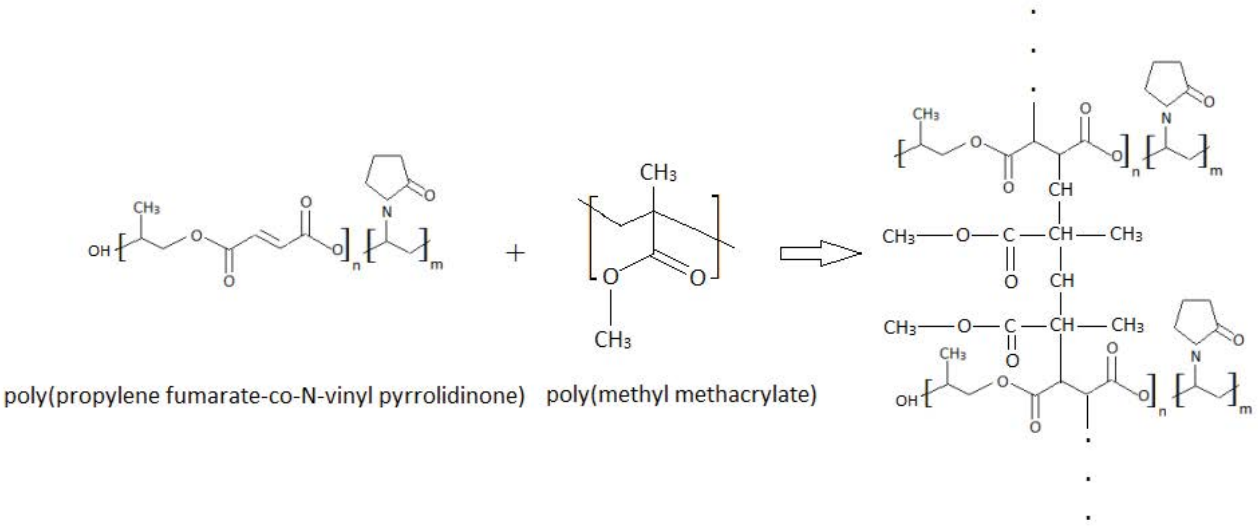

Fig. 1. Schematic representation of hydrogel synthesis.

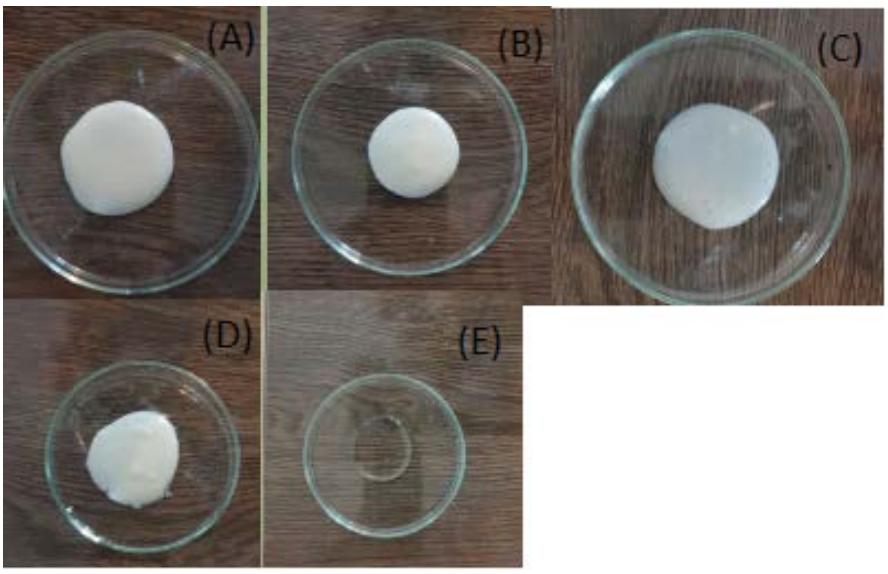

Fig. 2. Visual observation of hydrogel synthesized using different monomer ratios at room temperature [PPF/NVP (a) 100/0, (b) 90/10, (c) 80/20, (d) 70/30, and (e) 60/40].

Table 1
Molecular weights of copolymers

PPF/NVP molar ratio	M_n (g/mol)	M_w (g/mol)	PDI
100/0	1,095	1,600	1.46
90/10	935	1,432	1.53
80/20	764	1,223	1.6
70/30	565	978	1.73

property of the hydrogel, increasing the rate of response of the hydrogel to the external temperature difference.

Fig. 7 shows the DSC profiles of synthetic hydrogels with various molar ratios of two polymers. The VPTT values of the poly(PPF-*co*-NVP) hydrogels synthesized with PPF/NVP molar ratios of 100/0, 90/10, 80/20, and 70/30 were found to be 25.2°C, 25.8°C, 26.5°C, and 27.6°C respectively. It is clear that as the NVP molar concentration was increased, the VPTT of hydrogel was shifted to the higher temperature. This change occurs due to the addition of hydrophilic NVP polymer which aids the formation of hydrogel with higher hydrophilicity property. VPTT data of the synthesized hydrogels are summarized in Table 3. With increasing NVP content, the hydrophilic/hydrophobic interaction of the hydrogel shifted more toward the hydrophilic nature and its corresponding VPTT has shifted on the higher side [34].

Fig. 8 shows the equilibrium swelling ratio of poly(PPF-*co*-NVP) hydrogels as a function of the external temperature in distilled water. As shown in Fig. 8, addition of NVP polymer from 10 to 30 mole percentage gently improves the equilibrium swelling ratio. As can be seen in Fig. 8, the equilibrium swelling ratio of all hydrogels reduces with temperature, which is rapid around the VPTT and then follow by a more gradual decline until become constant. These results might be explained by the fact that the incorporation of NVP polymer into the copolymer backbone chain would change the hydrophobic/hydrophilic balance of PPF hydrogels. The high hydrophilicity of NVP polymer causes an ascend trend on equilibrium swelling ratio of hydrogels. The increase of the NVP content will increase the hydrophilicity of the gel network. Therefore, the equilibrium swelling ratio of hydrogels is increased.

Also at low temperatures (below VPTT), the hydrophilic groups on polymer structure interacted strongly with water molecules and the polymer swells. By increasing temperature more than VPTT, the hydrophobic interactions on the surface of hydrogels between hydrophobic groups strengthened, so phase separation occurs, polymer shrinks, and water was released quickly. This temperature dependence property can be used for draw solution recovery.

The deswelling kinetic of PPF hydrogel is shown in Fig. 9, from which it can be seen that the response rate of hydrogel (PPF/NVP:70/30) has descending trend. It is clear that the hydrogel lost 81% water within 2 min. afterward the deswelling kinetic is decreased gradually until become constant.

By transferring the hydrogel from de-ionized water of 20°C to de-ionized water of 50°C the reinforced hydrophobic interactions on the surface region causes water to release quickly.

3.2. Osmotic pressure and relative viscosity

The osmotic pressures of poly(PPF-*co*-NVP) solutions of different concentrations are measured and shown in Table 4, and compared with those of NaCl solutions. In general, the osmotic pressure is increased with incorporation of NVP polymer in the hydrogel as draw solution. At the same concentration, the osmotic pressures follow an order of poly (PPF-*co*-NVP): 70/30 > poly(PPF-*co*-NVP): 80/20 > poly(PPF-*co*-NVP): 90/10 > NaCl, and a highest osmotic pressure of 134.5 bar is obtained for synthetic hydrogel with hydrogel of PPF/NVP:70/30 molar ratio.

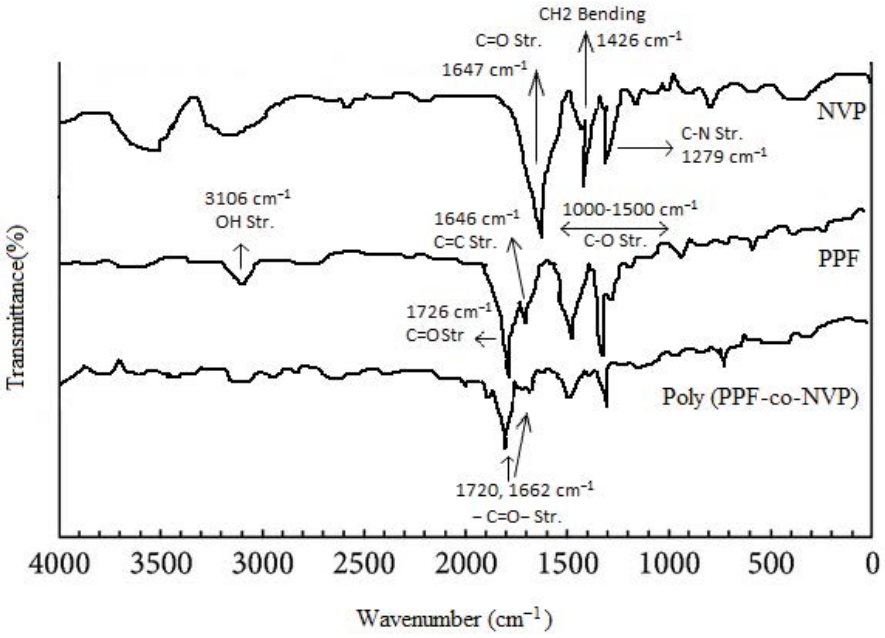

Fig. 3. FTIR spectra of NVP, PPF, and hydrogel of poly(PPF-*co*-NVP).

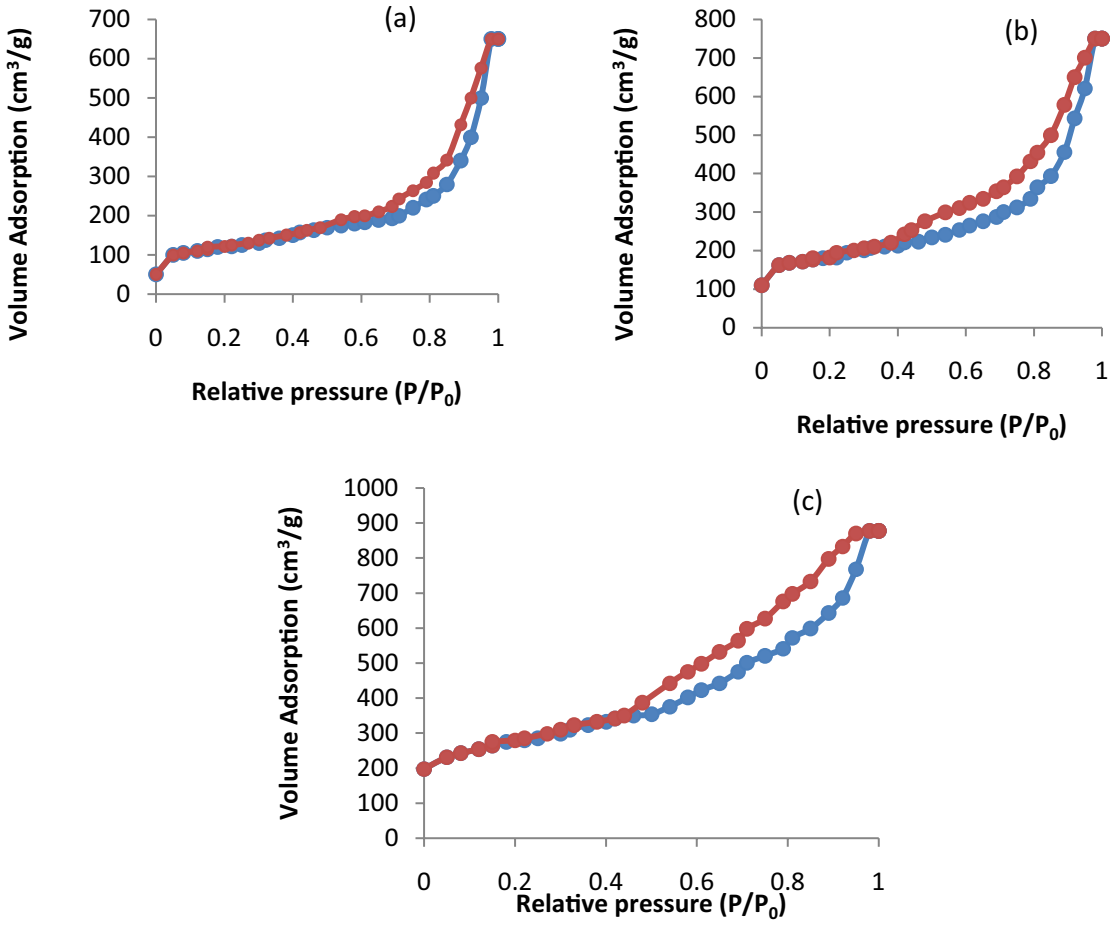

Fig. 4. Nitrogen adsorption–desorption isotherms of synthesized hydrogels, PPF/NVP molar ratio (a) 90/10, (b) 80/20, and (c) 70/30 (and correspond to adsorption and desorption branches, respectively).

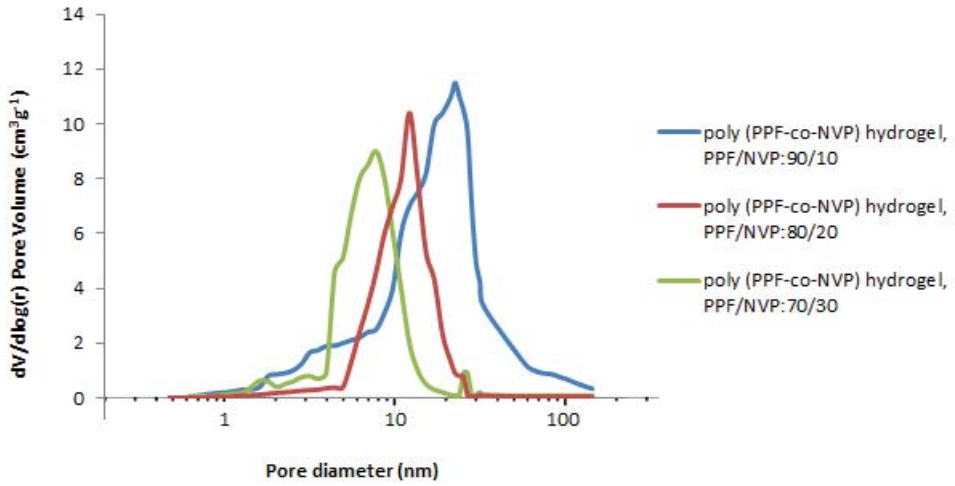

Fig. 5. Pore size distribution of synthesized hydrogels.

Table 2
Structural parameters of synthesized hydrogels

Hydrogel	Total surface area (m^2/g)	Total pore volume (cm^3/g)	Average pore diameter (nm)
Poly(PPF-*co*-NVP), PPF/NVP:90/10	59.4	0.45	26.3
Poly(PPF-*co*-NVP), PPF/NVP:80/20	83.2	0.42	10.9
Poly(PPF-*co*-NVP), PPF/NVP:70/30	112.6	0.39	8.7

The relative viscosities of synthetic hydrogels and NaCl solutions are also investigated and shown in Fig. 10. As shown Fig. 10, relative viscosities of all synthetic solutions increase significantly with the concentration increase, but this shows slow increasing trends with the concentration increase when the concentration is relatively less than 1 mol/L due to low intermolecular forces [35]. Due to the ICP effect caused by viscos solution, a high viscosity of the draw solution is not suitable for the FO application.

With the desirable properties of the high osmotic pressure and the low viscosity, synthetic hydrogel solutions at concentration of less than 1.5 mol/L are therefore expected to exhibit good FO performance as potential draw solutions.

3.3. Evaluation of FO performance

Fig. 11 shows the FO performance of a laboratory scale cross flow FO membrane against deionized water and synthetic brackish water as feed solutions. It can be observed that, the water flux increases with the increase in the concentration from 0.5 to 2 mol/L for all draw solutions because of the higher osmotic pressure.

In all draw solutions, the water flux increasing is rapid at low concentrations but slows down at higher concentrations. This might be because of the severer ICP effect and the lower dissociation degree of the solution with a higher concentration. Among draw solution that studied in this study poly (PPF-*co*-NVP): 70/30 draw solution exhibits a higher water flux of 29.3 LMH in FO mode, which could be explained to its higher osmotic pressure and lower viscosity than those of poly(PPF-*co*-NVP): 100/0, 90/10, and 80/20 solution as shown in Fig. 11.

With this much of water flux, if the solute leakage (J_s) across the membrane is considered, it can be seen from Fig. 12 that the RSF for 0.5 M NaCl as DS was 4.4 g MH while it is only 0.7 g MH for the poly(PPF-*co*-NVP): 70/30 draw solution. The maximum experimental RSF for the poly (PPF-*co*-NVP) draw solutions was even less than 1.4 g MH.

Basically, higher molecular weights of the draw solute are more desirable, because the former generally corresponds to a lower solute leakage, whereas the latter brings out a higher water flux in the DO process [36]. Increasing the weight percent PPF in the copolymer increases the molecular weight of copolymer (Table 1).

A very lower value of J_s in case of poly(PPF-*co*-NVP): 100/0 draw solution shows a higher molecular weight which suppressed solute diffusion across the membrane. Membrane fouling is one of the RSF results that lead to decline the flux.

The FO performance of the novel draw solution was also checked against synthetic brackish water containing 4.0 wt.% NaCl solution as feed water (Fig. 13). The results indicated that the water flux decreased considerably when brackish water replaced DI water as the feed solution as the osmotic pressure exerted by brackish water reduced the net driving force across the membrane, leading to a reduction in the water flux [12].

Though, the water permeation flux is reduced with brackish water as feed water but still the poly(PPF-*co*-NVP) draw solution have enough osmotic driving force to produce

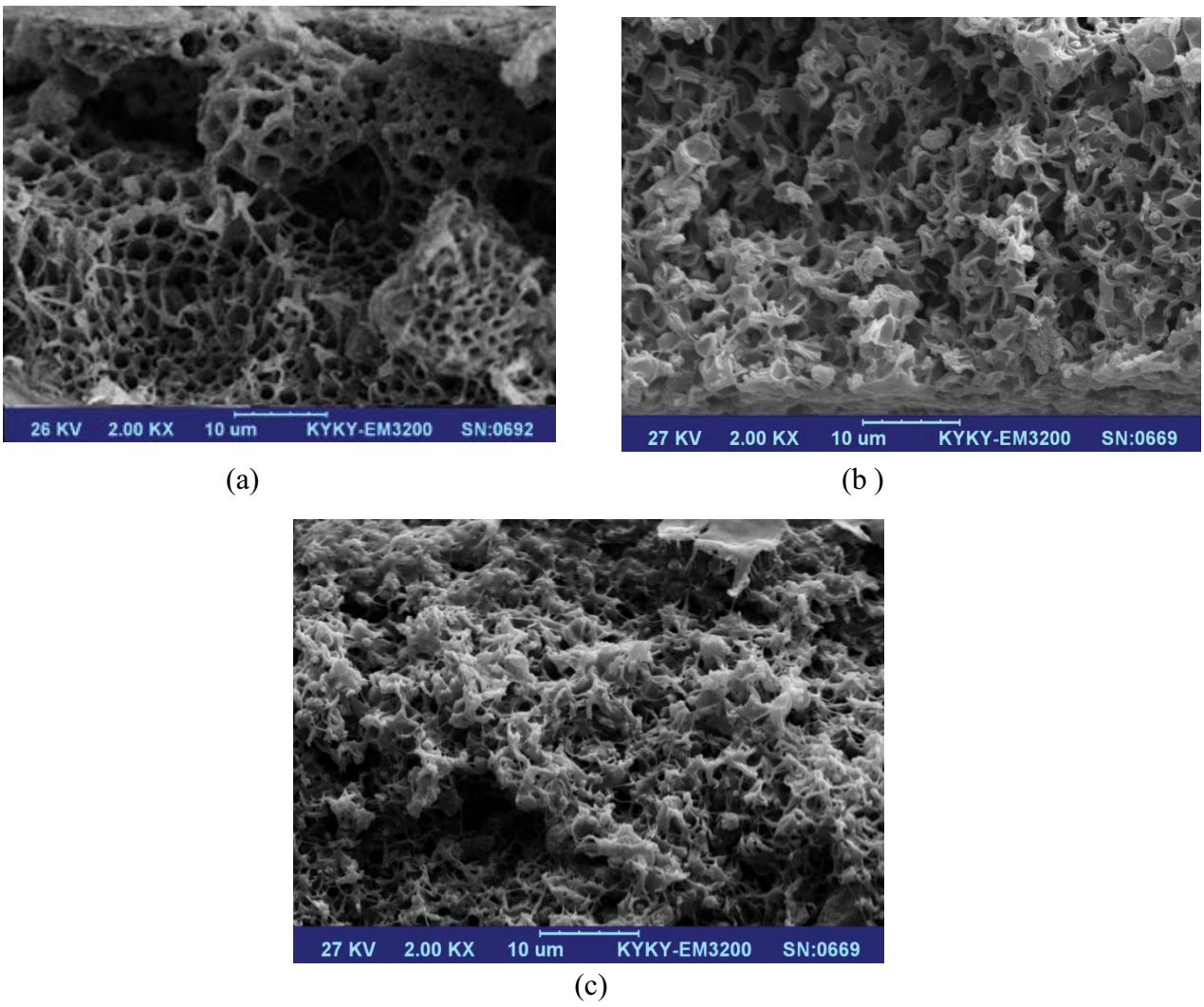

Fig. 6. SEM images of the synthesized hydrogels, PPF/NVP molar ratio (a) 90/10, (b) 80/20, and (c) 70/30.

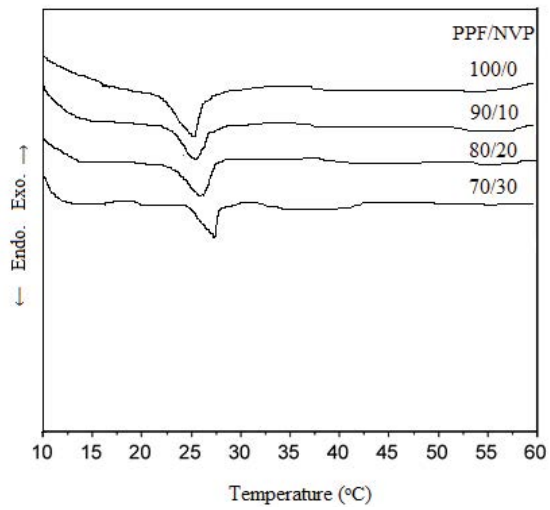

Fig. 7. DSC curves of poly(PPF-*co*-NVP) hydrogels with various content of NVP and the VPTT as a function of molar ratio of PPF/NVP.

Table 3
VPTT data for hydrogels

Sample	PPF/NVP molar ratio	VPTT (°C)
1	100/0	25.2 ± 0.1
2	90/10	25.8 ± 0.2
3	80/20	26.5 ± 0.2
4	70/30	27.6 ± 0.1

a water flux of 13.4 LMH at a draw solute concentration of only 0.5 mol/L indicating that the new draw solution was still osmotically strong enough to desalinate brackish with even higher salinity level (4.0 wt.% NaCl solution).

4. Conclusion

The novel temperature responsive hydrogel of poly (PPF-*co*-NVP) has been synthesized. The incorporation of NVP into the backbone chain of PPF affects the response to

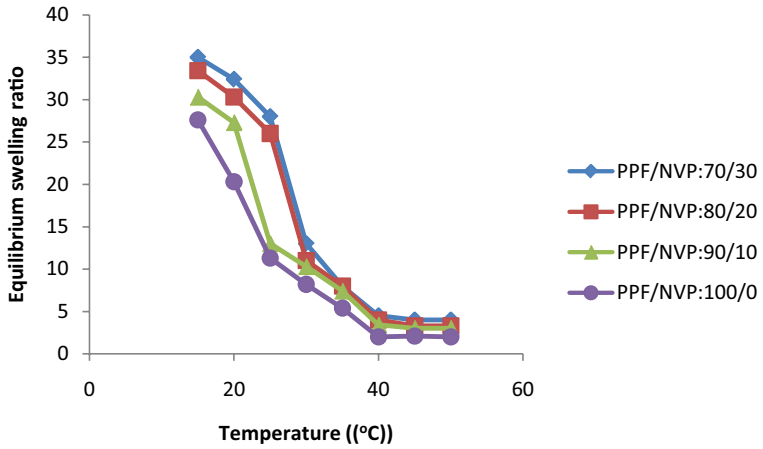

Fig. 8. Temperature dependence of equilibrium swelling ratio of synthetic hydrogels. (Summary of protocol: initially gel samples were incubated in DI water for at least 24 h at room temperature). Then 30 mL of dilute draw solution was transferred into the centrifuge tube and placed in a water bath. The solution was heated at different temperatures of 15°C up to 50°C. Time taken for complete phase separation at each temperature was determined. When the draw solution was heated above its VPTT, a clear liquid-liquid phase separation appeared which formed a hydrogel-rich phase and water-rich phase. After that the hydrogel was removed from the bath and the weight of the gel was recorded at 5°C intervals after blotting the excess surface water with moistened Whatman #1 filter paper. The dry weight of the hydrogel was measured after drying it under vacuum at room temperature. Then, the equilibrium swelling ratio was calculated by Eq. (1).

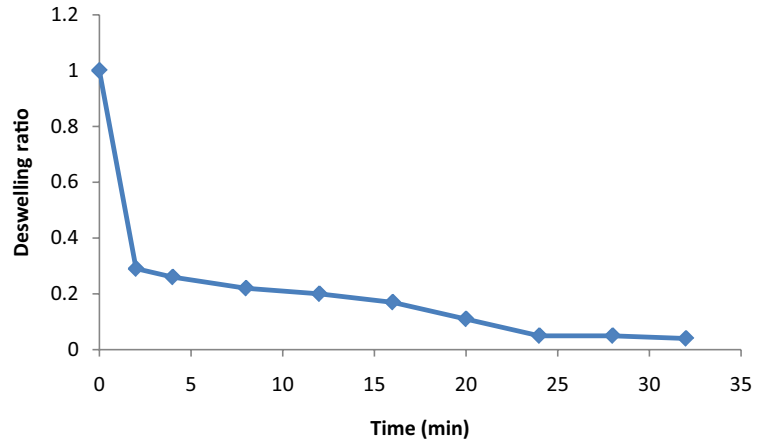

Fig. 9. Deswelling kinetics of the synthetic hydrogel (PPF/NVP: 70/30).

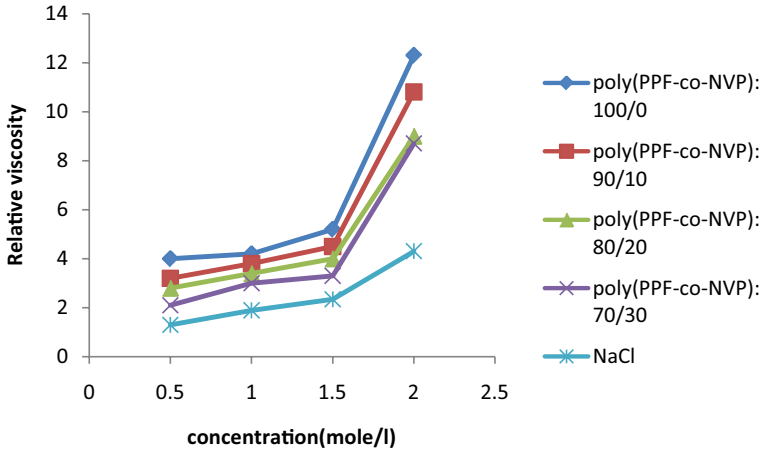

Fig. 10. Relative viscosities of draw solutions at various concentrations (temperature: 25°C ± 0.5°C).

Table 4
Osmotic pressure of synthetic hydrogels and sodium chloride solutions

	Osmotic pressure				
Concentration (M)	Poly(PPF-*co*-NVP): 100/0	Poly(PPF-*co*-NVP): 90/10	Poly(PPF-*co*-NVP): 80/20	Poly(PPF-*co*-NVP): 70/30	Sodium chloride
0.5	19.3	21.23	28.6	32.3	17.43
1	45.4	58.3	66.4	72.4	41.85
1.5	59.6	79.2	81.2	120.2	65.1
2	103.4	118.5	124.3	134.5	100.02

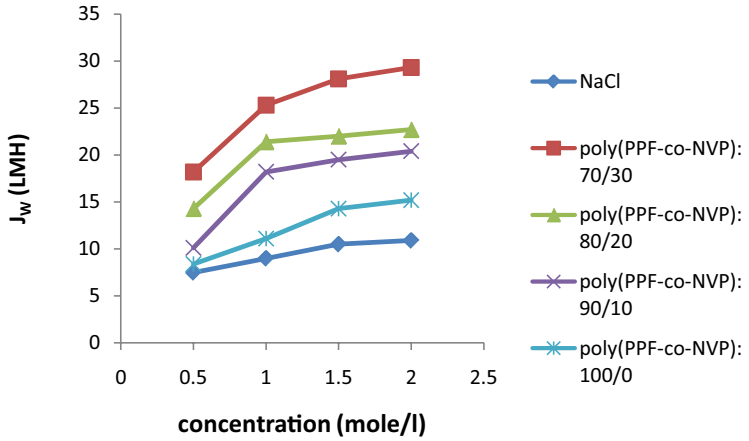

Fig. 11. Water flux against various concentrations of hydrogel. Experimental conditions: various concentrations of hydrogels as the draw solution, DI water as feed solution, temperature of 25°C ± 0.5°C and cross-flow velocities of 20 L/h on both sides of the FO membrane. Data were obtained from at least three tests on independent samples.

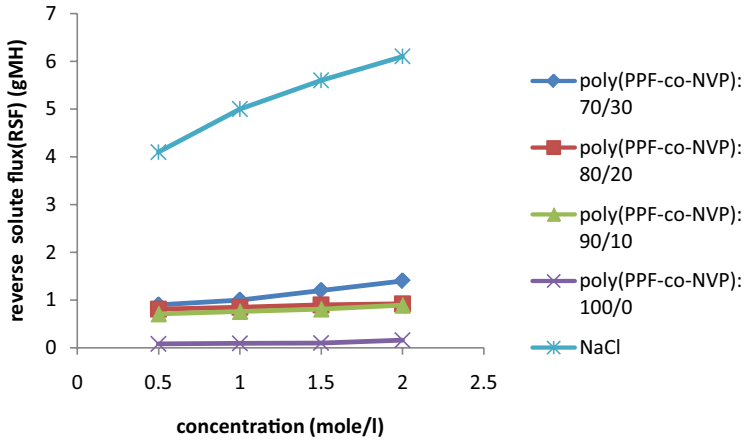

Fig. 12. Reverse solute flux against various concentrations of hydrogel. Experimental conditions: various concentrations of hydrogels as the draw solution, DI water as the feed solution, and cross-flow velocities of 20 L/h on both sides of the FO membrane. Data were obtained from at least three tests on independent samples.

the temperature. Also NVP concentration had significant effect on the time of gelation and the stability of the hydrogels. SEM analysis showed an increased pore structure and interconnectivity between pores as NVP concentration was increased. By increasing NVP molar concentration, the VPTT of hydrogel was shifted to the higher temperature which is confirmed by DSC analysis. The rate of change of swelling ratio with respect to the temperature was observed to be less below VPTT and it was more above VPTT of the hydrogels. Among draw solution that studied in this study poly (PPF-*co*-NVP): 70/30 draw solution exhibits a higher water flux of 29.3 LMH when DI water was used as the feed

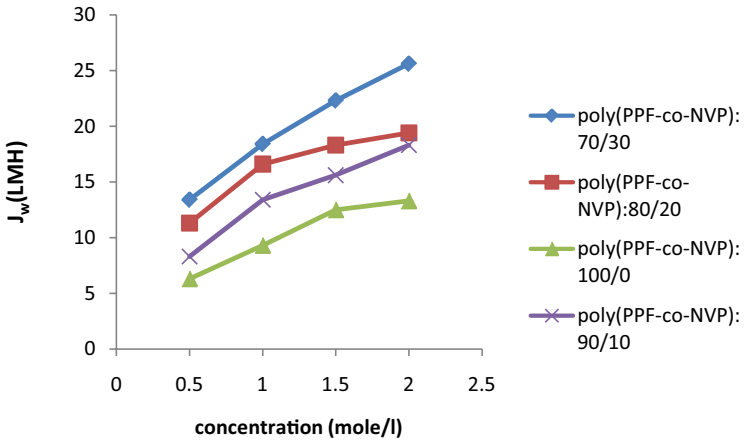

Fig. 13. Water flux against various concentrations of hydrogel. Experimental conditions: various concentrations of hydrogels as the draw solution, brackish water as feed solution, and cross-flow velocities of 20 L/h on both sides of the FO membrane. Data were obtained from at least three tests on independent samples.

solution in FO process, which could be explained to its higher osmotic pressure and lower viscosity than those of poly (PPF-*co*-NVP): 100/0, 90/10, and 80/20 solution.

The RSF with the concentration of 0.5 mole/L of poly(PPF-*co*-NVP): 70/30 within this work was 0.7 g MH only which is negligible as compared to 0.5 M NaCl as draw solution. Results showed that the new draw solutions developed in this work could be an appropriate candidate for the temperature assisted forward osmosis based desalination process.

References

[1] A. Achilli, T.Y. Cath, E.A. Marchand, A.E. Childress, The forward osmosis membrane bioreactor: a low fouling alternative to MBR processes, Desalination, 239 (2009) 10–21.
[2] Y. Li, Y. Zhao, E. Tian, Y. Ren, Preparation and characterization of novel forward osmosis membrane incorporated with sulfonated carbon nanotubes, RSC Adv., 8 (2018) 41032–41039.
[3] J.R. McCutcheon, R.L. McGinnis, M. Elimelech, Desalination by ammonia-carbon dioxide forward osmosis: influence of draw and feed solution concentrations on process performance, J. Membr. Sci., 278 (2006) 114–123.
[4] T.Y. Cath, A.E. Childress, M. Elimelech, Forward osmosis: principles, applications, and recent developments, J. Membr. Sci., 281 (2006) 70–87.
[5] S.F. Zhao, L. Zou, C.Y. Tang, D. Mulcahy, Recent developments in forward osmosis: opportunities and challenges, J. Membr. Sci., 396 (2012) 1–21.
[6] Q. Long, G. Qi, Y. Wang, Evaluation of renewable gluconate salts as draw solutes in forward osmosis process, ACS Sustainable Chem. Eng., 4 (2016) 85–93.
[7] Q. Ge, T.S. Chung, Hydroacid complexes: a new class of draw solutes to promote forward osmosis (FO) processes, Chem. Commun., 49 (2013) 8471–8473.
[8] Q.W. Long, Y. Wang, Novel carboxyethyl amine sodium salts as draw solute with superior forward osmosis performance, AIChE J., 62 (2015) 1226–1235.
[9] L. Chekli, S. Phuntsho, H.K. Shon, S. Vigneswaran, J. Kandasamy, A. Chanan, A review of draw solutes in forward osmosis process and their use in modern applications, Desal. Water Treat., 43 (2012)167–184.
[10] A. Achilli, T.Y. Cath, A.E. Childress, Selection of inorganic based draw solutions for forward osmosis applications, J. Membr. Sci., 364 (2010) 233–241.
[11] H.Y. Ng, W. Tang, Forward (direct) osmosis: a novel and prospective process for brine control, Water Environ. Fed., 2006 (2006) 4345–4352.
[12] H.T. Nguyen, N.C. Nguyen, S.S. Chen, H.H. Ngo, W. Guo, C.W. Li, A new class of draw solutions for minimizing reverse salt flux to improve forward osmosis desalination, Sci. Total Environ., 538 (2015) 129–136.
[13] D. Li, H. Wang, Smart draw agents for emerging forward osmosis application, J. Mater. Chem. A, 1 (2013) 14049–14060.
[14] T. Alejo, M. Arruebo, V. Carcelen, V.M. Monsalvo, V. Sebastian, Advances in draw solutes for forward osmosis: hybrid organic-inorganic nanoparticles and conventional solutes, Chem. Eng. J., 309 (2017) 738–752.
[15] Y. Cai, X.M. Hu, A critical review on draw solutes development for forward osmosis, Desalination, 391 (2016) 16–29.
[16] D. Roy, M. Rahni, P. Pierre, V. Yargeau, Forward osmosis for the concentration and reuse of process saline wastewater, Chem. Eng. J., 287 (2016) 277–284.
[17] Q. Ge, F. Fu, T.S. Chung, Ferric and cobaltous hydroacid complexes for forward osmosis (FO) processes, Water Res., 58 (2014) 230–238.
[18] S. Zhao, L. Zou, D. Mulcahy, Brackish water desalination by a hybrid forward osmosis – nanofiltration system using divalent draw solute, Desalination, 284 (2012) 175–181.
[19] Q. Ge, J. Su, G.L. Amy, T.S. Chung, Exploration of polyelectrolytes as draw solutes in forward osmosis processes, Water Res., 46 (2012) 1318–1326.
[20] D. Zhao, P. Wang, Q. Zhao, N. Chen, X. Lu, Thermoresponsive copolymer-based draw solution for seawater desalination in a combined process of forward osmosis and membrane distillation, Desalination, 348 (2014) 26–32.
[21] R. Ou, Y. Wang, H. Wang, T. Xu, Thermo-sensitive polyelectrolytes as draw solutions in forward osmosis process, Desalination, 318 (2013) 48–55.
[22] A.J. Domp, J. Kost, D.M. Wiseman, Handbook of Biodegradable Polymers, Harwood Academic Publishers, Amsterdam, 1997.
[23] D. Li, X. Zhang, J. Yao, G.P. Simon, H. Wang, Stimuli-responsive polymer hydrogels as a new class of draw agent for forward osmosis desalination, Chem. Commun., 47 (2011) 1710–1712.
[24] S. Wang, D.H. Kempen, M.J. Yaszemski, L. Lu, The roles of matrix polymer crystallinity and hydroxyapatite nanoparticles in modulating material properties of photo-crosslinked composites and bone marrow stromal cell responses, Biomaterials, 30 (2009) 3359–3370.
[25] L.J. Suggs, R.G. Payne, M.J. Yaszemski, L.B. Alemany, A.G. Mikos, *Synthesis* and *characterization* of a block copolymer consisting of poly(propylene fumarate) and poly(ethylene glycol), Macromolecules, 30 (1997) 4318–4323.
[26] E.S. Dragan, A.I. Cocarta, M. Gierszewska, Designing novel macroporous composite hydrogels based on methacrylic acid

copolymers and chitosan and *in vitro* assessment of lysozyme controlled delivery, Colloids Surf., B, 139 (2016) 33–41.
[27] B. Maheswari, P.E. Jagadeesh Babu, M. Agarwal, Role of N-vinyl-2-pyrrolidinone on the thermoresponsive behavior of PNIPAm hydrogel and its release kinetics using dye and vitamin-B12 as model drug, J. Biomater. Sci., Polym. Ed., 25 (2014) 269–286.
[28] J.Y. Park, W.W. Jeong, J.W. Nam, J.H. Kim, K. Chon, E. Lee, H.S. Kim, A. Jang, An analysis of the effects of osmotic backwashing on the seawater reverse osmosis process, Environ. Technol., 35 (2014) 1455–1461.
[29] Y. Xu, X. Peng, C.Y. Tang, Q.S. Fu, S. Nie, Effect of draw solution concentration and operating conditions on forward osmosis and pressure retarded osmosis performance in a spiral wound module, J. Membr. Sci., 348 (2010) 298–309.
[30] Y.J. Choi, J.S. Choi, H.J. Oh, S. Lee, D.R. Yang, J.H. Kim, Toward a combined system of forward osmosis and reverse osmosis for seawater desalination, Desalination, 247 (2009) 239–246.
[31] J.R. McCutcheon, R.L. McGinnis, M. Elimelech, Desalination by ammonia–carbon dioxide forward osmosis: Influence of draw and feed solution concentrations on process performance, J. Membr. Sci., 278 (2006) 114–123.
[32] M. Garcia-Castello, J.R. McCutcheon, M. Elimelech, Performance evaluation of sucrose concentration using forward osmosis, J. Membr. Sci., 338 (2009) 61–66.
[33] N.T. Hancock, T.Y. Cath, Solute coupled diffusion in osmotically driven membrane processes, Environ. Sci. Technol., 43 (2009) 6769–6775.
[34] B. Vernon, S.W. Kim, Y.H. Bae, Thermoreversible copolymer gels for extracellular matrix, J. Biomed. Mater. Res., 51(2000) 69–79.
[35] H.S. Yoo, M.L. Fishman, A.T. Hotchkiss, H.G. Lee, Viscometric behavior of high-methoxy and low-methoxy pectin solutions, Food Hydrocolloids, 20 (2006) 62–67.
[36] M. Narimani, M. Arjmand, S.M. Tabatabaee Ghomsheh, A. Safekordi, Evaluation of direct osmosis at high salinities method by renewable lactate salts as draw solutes in RO membrane cleaning, Desal. Water Treat., 79 (2018) 1–11.